DETERMINATION OF AERODYNAMIC COEFFICIENTS NECESSARY FOR THE CONTROL OF MAVs

M.Sc. Kambushev M. PhD.[1], M.Sc. Biliderov S. PhD.[1]

Faculty of Aviation, Dolna Mitropolia – National Military University, Veliko Turnovo, Bulgaria [1]

m_kambushev@yahoo.com, biliderow_ss@yahoo.com

Abstract: *The present paper examines the use of free software to determine the aerodynamic coefficients of the selected MAVs. The resulting ratios and aerodynamic forces and momentums are tested for their applicability in the controlling of this type of aircrafts.*

Keywords: MINI AIR VECHICLES (MAVs), AERODYNAMIC COEFFICIENTS, AERODYNAMIC FORCES AND MOMENTUMS, FREE SOFTWARE, CONTROL OF MAVs

ОПРЕДЕЛЯНЕ НА АЕРОДИНАМИЧНИ КОЕФИЦИЕНТИ НЕОБХОДИМИ ЗА УПРАВЛЕНИЕТО НА MAVs

маг. инж. Камбушев М., д-р, маг. инж. Билидеров С., д-р [1]

Факултет "Авиационен", Долна Митрополия – Национален Военен Университет, Велико Търново, България [1]

m_kambushev@yahoo.com, biliderow_ss@yahoo.com

Abstract: *В настоящият доклад се разглежда използването на свободен софтуер за определяне на аеродинамичните коефициенти на избран MAVs. Получените коефициенти, както и аероднамичните сили и моменти са изследвани за тяхната приложимост при управлението на този тип летателни апарати.*

Keywords: МИНИ БЕЗПИЛОТНИ ЛЕТАТЕЛНИ АПАРАТИ (МБЛА), АЕРОДИНАМИЧНИ КОЕФИЦИЕНТИ, АЕРОДИНАМИЧНИ СИЛИ И МОМЕНТИ, СВОБОДЕН СОФТУЕР, УПРАВЛЕНИЕ НА МБЛА

Error! No sequence specified.. Introduction

For each specific task related to the use of unmanned aerial vehicles (UAV), different planar designs and algorithms for automatic control are applied. In intelligence and reconnaissance missions, the proper construction of the UAV is in the field of mini air vehicles (MAVs). Frequently used structure is in the shape of a flying wing.

When there are templates of complete flyer structures, it is necessary, together with their assembly, to carry out theoretical researches on the possibility of reaching the target of the mission. The main problems come from the fact that nothing can be learned about the flying characteristics and operational capabilities of the chosen MAV from the templates. For these characteristics, it is necessary to examine the profiles from which the MAV is built, as well as the aerodynamic coefficients entering the expressions for finding the aerodynamic forces and the momentums acting in the rigid body MAV. The forces and momentums thus found are involved in the complete mathematical model [4], [8] of the MAV, from which the appropriate control is synthesized [3], [5].

A suitable solution for the chosen case is the use of specialized software for studying in a profile and plan of a flying wing type MAV. Many such software platforms are available on the market, ranging from free to fairly expensive. All of them have their advantages, but particularly suited for the purpose, in terms of price and functionality, is the software product XFLR5 [7], [9], [11].

2. Examination of aerodynamic characteristics

For the purpose of the study, a flying wing type MAV was selected with the corresponding profile and plan dimensions [6]. After the wing has been fabricated, the dimensions of the obtained profiles are taken and the MAV is drawn in the middle of the XFLR5. The result is shown in Fig.1.

The profiles from which the MAV is constructed are three and after the measurement and interpolation, in relative dimensions they have the shapes shown in Fig.2.
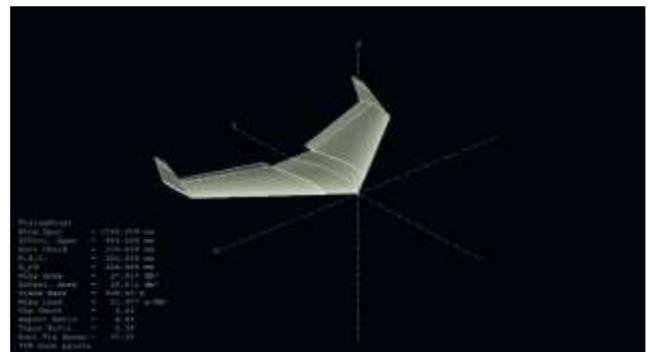

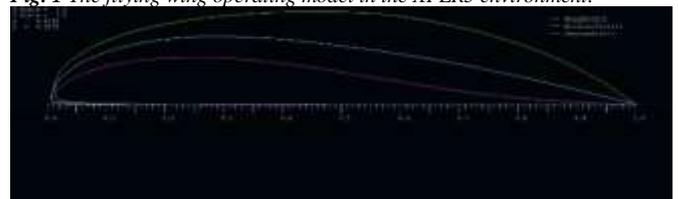**Fig. 1** *The flying wing operating model in the XFLR5 environment.*

Fig. 2 *The working plan of profiles in the XFLR5 environment.*

The profiles thus obtained have the following geometry:

1. The main profile named Osnoven profil - Max thickness 11.6% at 29.7% chord; Max camber 4.5% at 31.9% chord;

2. the middle profile named Mejdinen Profil - Max thickness 8.1% at 27.2% chord; Max camber 3.2% at 25.2% chord;

3. The end profile named Kraen Profil - Max thickness 15.8% at 47.5% chord; Max camber 6.2% at 54% chord.

For the study of the profiles from which the wing is made, the speeds for which the MAV is designed are set, and they are in the range V = 1 ÷ 20 m/s (3,6 ÷ 72 km/h). Also, the attack angle of the profile α = -50 ÷ 90 °is set. Fig.3 shows the results of the virtual air moving tunnel of the obtained profiles in the XFLR5 environment

at three selected speeds: $V_1 = 1$ [m/s]; $V_2 = 10$ [m/s]; $V_3 = 20$ [m/s] at specified attack angles α.

The results show (Fig. 3) that the lifting force for all three profiles is greatest for attack angles α = 20 ÷ 40 °, and the drag force is small at attack angles α = 0 ÷ 20 °. The aerodynamic quality of the angles of attack profiles is greatest at about α≈20°. The polar graph shows the same trend for all profiles when changing the speed and angle of attack. On Fig.3 it is seen that the main profile manifests a flow collapse at maximum speed, and for the end profile such a collapse is still observed at intermediate speeds.
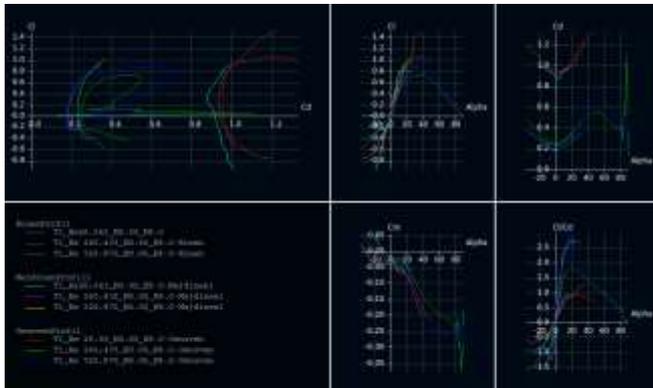

Fig. 3 *Exploring the profiles in the Direct flow analyze.*

For the profile to be stable in the airflow, the pitch momentum coefficient should be $c_m = 0$. For the profiles thus obtained, this coefficient is zero at negative attack angles.

On the basis of these profiles and the selected geometry in the plan of the flying wing MAV type, the planer is developed (Fig.1). In the XFLR5 environment at different velocities and angles of attack (Fig. 4) the dependencies for the coefficients of the aerodynamic forces (Fig.5) and momentums (Fig.6) are obtained.
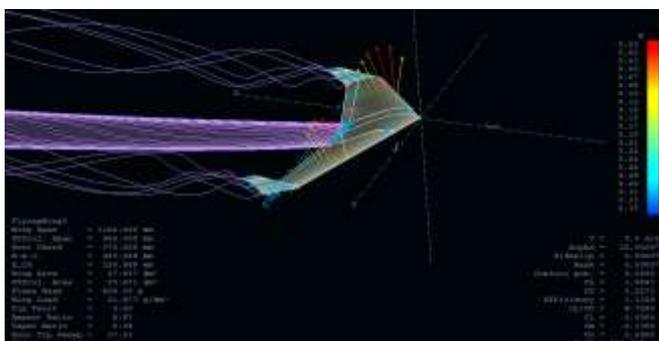

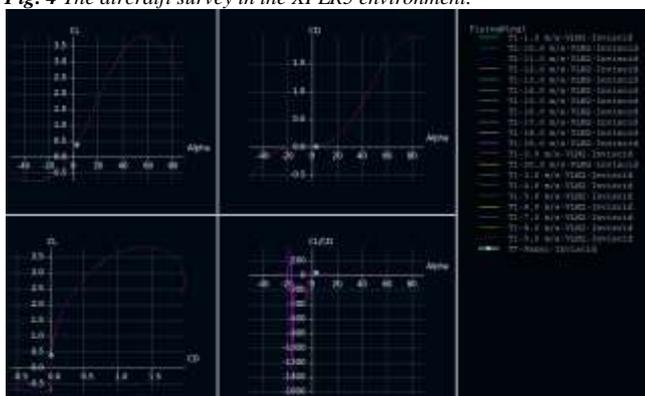**Fig. 4** *The aircratft survey in the XFLR5 environment.*

Fig. 5 *The aerodynamic coefficients, polar and airplane quality in the XFLR5 environment.*

On the Fig. 5 are depicted the dependencies of the coefficients of the lifting force, the drag resistance, the polar of the wing and its quality depending on the angle of attack. The dependencies show that at the angle α = 50 ÷ 70 ° the coefficient of lifting force c_y has the greatest value. By contrast, the drag coefficient c_d has the

greatest value at an angle α = 70 ÷ 90 °. The wing polar (Fig. 5) shows that the most favorable angle of attack is α = 14 ° and the critical attack angle is α = 56 °. From the MAV quality chart, it is seen that the highest quality is obtained at negative angles of attack.

On Fig. 6 is shown the dependence of the pitch momentum coefficient from the change in the angle of attack (magenta). From this dependence, it can be seen that the balancing angle of the attack is α = -7.3 °, which means that MAV balance is obtained at negative angles of attack.
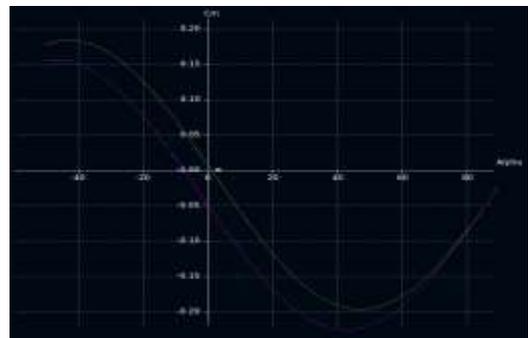

Fig. 6 *Obtaining the aerodynamic momentum coefficients in the XFLR5.*

For additional balancing of the plane, it is necessary to relocate the load masses to the geometric dimensions of the planer or to put the altitude control surfaces in the appropriate position. In this case, a balance is selected by changing the angle of the control surfaces with $\delta_в = 5°$. Fig. 6 shows the result of this control surfaces' adjustment, with the pitch momentum equal to zero at an angle of attack α = 1,14°. The control surfaces' adjustment also influences the aerodynamic coefficients as shown in Fig.7.

It can be seen from Figure 7 that the lifting force is greatest at attack angle α = 57°, and the drag coefficient is greatest at an angle of attack α = 70°. It is noted that both factors are smaller in amplitude following the change of the angle of the control surfaces. The angle of attack at zero lift force $α_{cy0} = -0,34°$, which is the expression of the coefficient of non-inductive resistance. It is evident from the graph of the polar in Fig.7 that after deflection of the rules, the quality of the MAV deteriorates slightly due to the displacement of the graph to the right and also to the slight increase of the inductive resistance. However, the maximum qualities of the wing are close (Fig.7).
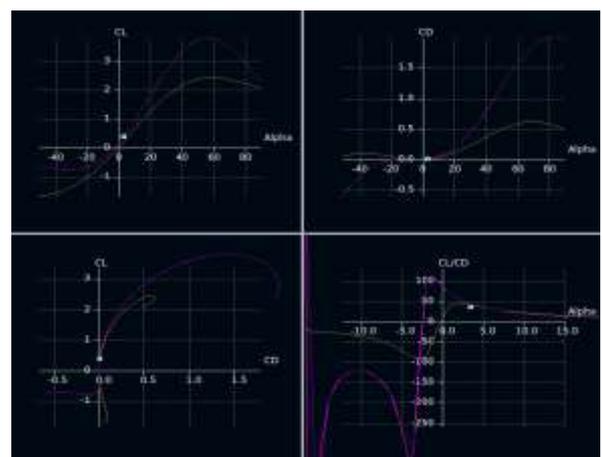

Fig. 7 *The aerodynamic coefficients after balancing with the rules of the altitude.*

The polar curve also shows the ability of the MAV to gain vertical velocity at negative or positive angles of attack. The curve at high elevation ratios indicates the possibility of the MAV to climb vertically at low horizontal velocities, and the smooth or abrupt transition refers to the rate of crushing when the flow is broken off. Fig. 8 a) shows the dependence of the vertical velocity on the angle of attack. It can be seen that when changing the angle α, MAV tends to increase its vertical velocity. Fig. 8 (b) shows the

tendency for the MAV to change its vertical speed when changing the horizontal at a fixed lift.

The asymmetry and the behavior of the polar in the half-plane of the negative force coefficients (Fig. 7) enables the MAV to perform inverted flights, and also provide information regarding the difference in the execution of figures in normal and inverted flight. It shows that the figures in the inverted flight are limited by the angle of attack.
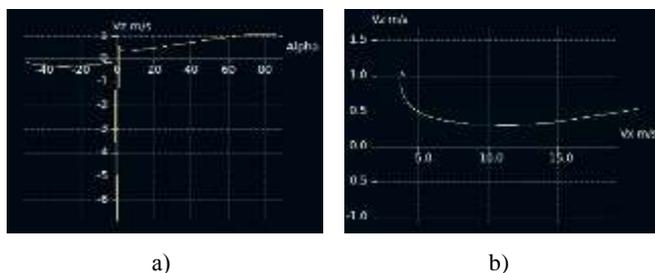

a)   b)

***Fig. 8** The ability of an MAV to climb or descend at different angles of attack.*

Three characteristic points are also defined on the MAV's polar. The first one is for the critical angle of the attack - $\alpha_{\kappa p}$. The critical angle of attack (Fig. 7) $\alpha_{\kappa p} = 59°$, at this angle the aircraft is held in the air at the minimum possible speed, which is useful for the landings. For the constructed MAV at weight $G = 0,609$ [kg], the lifting force in the vertical plane is obtained at a linear velocity $Vx = 3,714$ [m/s] (Fig.9a)). The safe lifting force must be less than the critical lifts at critical attack angles. It is obtained in the flight tests and lies within the limit of the lift coefficient when starting the transition and the maximum lifting force.
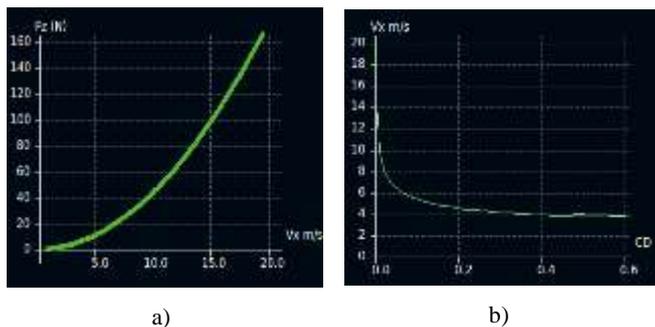

a)   b)

***Fig. 9** The ability of the MAV: a) to fly at critical attack angles; b) to fly at maximum speed.*

The next one is for the economic angle of the attack - $\alpha_{\text{икн}}$ (the most advantageous) in which the drag coefficient is minimal but different from zero, at this angle of attack, the inductive resistance is a half of the resistance of the airplane and the aircraft can fly at maximum speed (Fig. 9b)). At this angle, the deviation of the full aerodynamic force from the air flow direction is maximal. To find this polar point, the aerodynamic quality chart of the MAV is used (Fig.7). It shows that the most advantageous angle of attack is $\alpha = 2,5°$. For this angle, the lifting force significantly exceeds the drag coefficient and the linear velocity is $Vx = 14,15$ [m/s] (Fig. 9b)). With this speed, the MAV can fly at a fixed lift.

The last polar point is for the most favorable angle of attack (Fig. 7) $\alpha = 24°$. At this angle, the quality of MAV is the maximum $K = 9,3$. Then, only at this angle of attack for a certain height, it flies the farthest (windless) because the lift force is 9,3 times greater than the drag, and for 1 meter altitude the airplane will fly 9.3 [m] (if the air is still).

The polar of wing and its derivative - the aerodynamic quality, show virtually all the basic planning properties of the developed MAV. In order for this to happen, the wind speed needs to be 0,00 [m/s] (calm atmosphere), the airplane should not change its planning speed and its engine must be off. This feature of the MAV is useful when the engine shuts down into the air or when the battery capacity is exhausted.

Aside from the fact that the polar (Fig. 7) shows the planning properties of the MAV, it also determines the angle of planning, which is also the angle of the slope of the trajectory. From formula (1), it can be seen that the planning angle depends only on the aerodynamic output of the MAV.

$$tg\Theta_{\text{мин}} = \frac{1}{K_{\text{макс}}}$$

(1)

where $\Theta_{\text{мин}}$ is the angle of slope of the trajectory, $K_{\text{макс}}$ is the aerodynamic quality of the wing.

From formula (1), it is clear that the minimum planning angle is reached at the most favorable attack angle when the aerodynamic quality of the MAV is greatest. Any other planning angle is achieved either by a small angle of attack and a high velocity or at a great angle and low speed, or these are the first and second planning modes.

The polar of the speeds (Fig.8b) is also an indicator of the glide path. It defines the angle of the trajectory slope, the planning speeds and the vertical descent in a steady rectilinear flight. It is especially useful when the engine shuts down in flight. This graph also determines the most economical speed and the most favorable speed, which is $Vx = 4,7$ [m/s].

In the presence of wind, the planning distance changes because of the change in the flight speed of the flight and the angle of wind direction reference. If the graph of Fig. 8 (b) is shifted with the wind indicators, the characteristics of the current flight conditions are obtained for the MAV. Only the maximum, minimum, economy and best flight speeds are not changed.

Unlike the minimum flight speed, the maximum speed is limited by the thrust of the propelled engine propulsion system. For the determination of the maximum and minimum flight speeds it is assumed that the flying wing model is absolutely smooth and the thrust does not depend on the flight velocity, which is practically valid for the electric motor driven screws.

For the thrust of the engine-propeller system used [2], the graph in Fig.10 is valid. It was taken experimentally and processed with mathematical methods for smoothing.
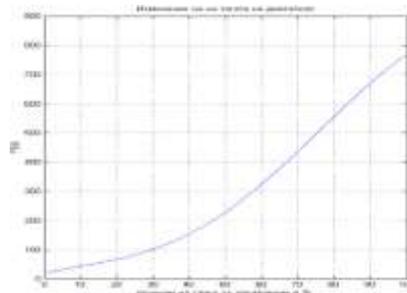

***Fig. 10.** The thrust of the engine-propeller system depends on the engine speed in function of the control.*

The static thrust of the engine-propeller system is taken at zero speeds of the air flow. A propeller (9*3,5) has been selected for the engine-propeller system operation. This propeller at maximum speed has a thrust of 760 grams or 7,453054 [N] at a flow rate of 9,5 [m/s].

Starting from the assumption that the propeller rotates at the same speed for the entire speed range, it results that for propeller 9*3.5 at zero flight speed the thrust will be 760 grams or 7,453054 [N], and at speed 9,5 [m/s] flight, the propeller will be screwed into the air and will not pull it back in any way, so the thrust will be zero.

This is the basis for Zhukovski's curves for the available and necessary trust. First, the graph of the dependence of the force of the linear drag on the linear velocity of the flight is constructed. In the MATLAB system then is imported the thrust data of the selected engine-propeller system and the overall graph shown in Fig.11 is drawn.

As can be seen from the graph in Fig.11, the model thus created will fly in a horizontal flight at Vx = 9,43 [m/s] and 99% thrust (Fig.10).
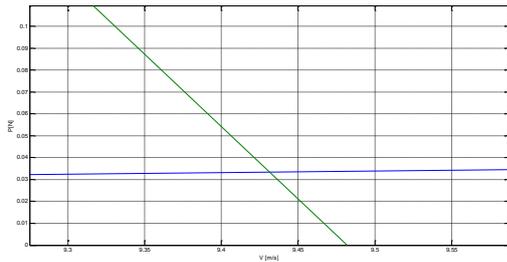

Fig. 11 Zhukovsky curves for the available and needed thrust.

For more accurate calculations of the engine-propeller system, simulations need to be made in specialized software products such as Qblade or MotoCalc.

The last speed of the flight is the cruise speed at which the MAV travels one kilometer with minimal fuel consumption. This speed allows for a maximum mileage with a fixed fuel volume where the ratio between the required thrust and the flight speed has a minimum value. At this speed, the MAV usually flies to the point of execution of the main mission, during reconnaissance missions, etc. This velocity (Fig. 11) is Vx = 9,5 [m/s].

3. Completing the mathematical model of MAVs

For the aerodynamic forces and momentums acting on this aircraft, the dependencies are shown in Fig.12 and Fig.13 (a). Fig. 12 depicts the dependencies for respectively: (a) the lift force; and (b) the drag force. Fig.13 shows respectively a) the pitching momentum and the developed MAV.
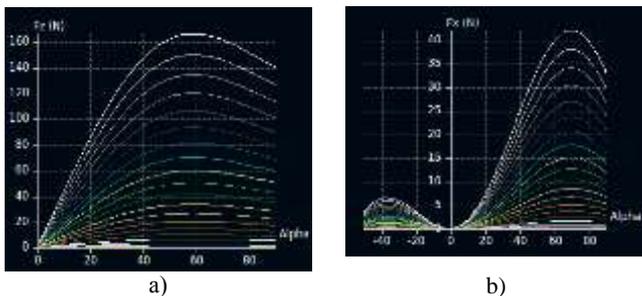

a)   b)

Fig. 12. The aerodynamic forces of lift and drag.
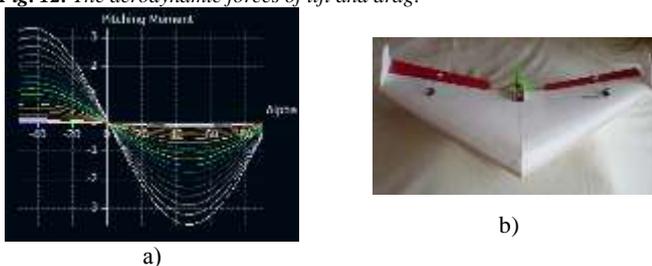

a)   b)

Fig. 13. The momentum of the pitch and the developed MAV.

The aerodynamic forces and momentums obtained in this way are designed to work with a mathematical model of motion of the MAV [10]:

changing the amount of movement:

$$(2) \quad \begin{aligned} m\left(\frac{dV_x}{dt} + \omega_y V_z - \omega_z V_y\right) &= \sum F_x \\ m\left(\frac{dV_y}{dt} + \omega_z V_x - \omega_x V_z\right) &= \sum F_y \\ m\left(\frac{dV_z}{dt} + \omega_x V_y - \omega_y V_x\right) &= \sum F_z \end{aligned}$$

where $V_x, V_y, V_z, \omega_x, \omega_y, \omega_z, \sum F_x, \sum F_y, \sum F_z$ is respectively the

projections of the velocity vector $\vec{V}$, angular velocity vector $\vec{\omega}$ and the external forces in the associated rigid body.

and to change the kinetic momentum:

$$(3) \quad \begin{aligned} I_x \frac{d\omega_x}{dt} + (I_z - I_y)\omega_y\omega_z + I_{zy}\left(\omega_{z^2} - \omega_{y^2}\right) - I_{xy}\frac{d\omega_y}{dt} - I_{xz}\frac{d\omega_z}{dt} + \omega_x\left(I_{yx}\omega_z - I_{zx}\omega_y\right) &= \sum M_x \\ I_y \frac{d\omega_y}{dt} + (I_x - I_z)\omega_z\omega_x + I_{zx}\left(\omega_{x^2} - \omega_{z^2}\right) - I_{yz}\frac{d\omega_z}{dt} - I_{yx}\frac{d\omega_x}{dt} + \omega_y\left(I_{zy}\omega_x - I_{xy}\omega_z\right) &= \sum M_y \\ I_z \frac{d\omega_z}{dt} + (I_y - I_x)\omega_x\omega_y + I_{xy}\left(\omega_{y^2} - \omega_{x^2}\right) - I_{zx}\frac{d\omega_x}{dt} - I_{zy}\frac{d\omega_y}{dt} + \omega_z\left(I_{xz}\omega_y - I_{yz}\omega_x\right) &= \sum M_z \end{aligned}$$

where: I_x, I_y, I_z are main momentums of inertia; I_{xy}, I_{xz}, I_{yz} are centrifugal inertia momentums; $\sum M_x, \sum M_y, \sum M_z$ are the sum of the projections of the momentum in the rigid body.

The model thus synthesized is designed to work in the flying-navigation complex of the MAV [1]

4. Conclusions and results

1. The profiles that are obtained after the assembly of the finished templates from which the MAV was made are studied.

2. Survey of the planner of the MAV was made. The results are described in the report.

3. The angular-speed restrictions for the MAV created were obtained.

4. Validation of the results which will be obtained in the aerodynamic tube and in real-life flights is pending.

5. Bibliography

[1] Бабич О., Обработка информации в навигационных комплексах. Москва 1991г.

[2] Билидеров С.С., М. М. Камбушев. Оценка на експериментално получени характеристики на системата двигател-витло за мини-безпилотни летателни апарати. ЮНС 2013, гр. Долна Митрополия, 2013г.

[3] Велева Е., Караколева С. Практикум по „Числени методи" с Matlab. РУ"Ангел Кънчев", Русе 2004г.

[4] Лысенко Н. М. Динамика полета. София, 1977, 638с

[5] Маджаров Н. Е. Линейни системи за управление. София, 1998,208с.

[6] Некрасов В. И.,А. Е. Викторов. Практическая аэродинамика учебных реактивных самолетов. София, 1987,246с.

[7] A. Deperrois: About performance and stability analysis using XFLR5 (November 201) <https://www.scribd.com/doc/101229735/XFLR5-and-Stability-Analysis> 01.05.2017

[8] Kambushev M., Biliderov S., Varbanov Y. Synthesis and study of the mathematical model of a tricopter. AFASES 2016.

[9] Martin Willner: A tutorial for XFLR5 version 1 <https://www.scribd.com/document/40661331/XFLR5-Tut-v1> 01.05.2017

[10] Stevens B.L., Lewis F. L. Aircraft control and simulation. John Wiley&Sons,2003.

[11] Guidelines for XFLR5 <https://osdn.net/projects/sfnet_xflr5/downloads/Guidelines.pdf/> 01.05.2017